ResearchGate

See discussions, stats, and author profiles for this publication at: https://www.researchgate.net/publication/236336675

Effect of Colloidal Substrate Curvature on pH-Responsive Polyelectrolyte Brush Growth

ARTICLE *in* LANGMUIR · APRIL 2013

Impact Factor: 4.46 · DOI: 10.1021/la4004092 · Source: PubMed

CITATIONS
7

READS
22

6 AUTHORS, INCLUDING:

Grant B Webber
University of Newcastle
51 PUBLICATIONS **782** CITATIONS
SEE PROFILE

Steve Edmondson
The University of Manchester
38 PUBLICATIONS **1,399** CITATIONS
SEE PROFILE

Erica J Wanless
University of Newcastle
81 PUBLICATIONS **2,514** CITATIONS
SEE PROFILE

Available from: Erica J Wanless
Retrieved on: 02 February 2016

Langmuir

Article

pubs.acs.org/Langmuir

Effect of Colloidal Substrate Curvature on pH-Responsive Polyelectrolyte Brush Growth

Benjamin T. Cheesman,[†] Alexander J. G. Neilson,[†] Joshua D. Willott,[†] Grant B. Webber,[†] Steve Edmondson,[‡] and Erica J. Wanless*[,†]

[†]Priority Research Centre for Advanced Particle Processing and Transport, University of Newcastle, Callaghan, NSW 2308, Australia

[‡]Department of Materials, Loughborough University, Loughborough, LE11 3TU, United Kingdom

Supporting Information

ABSTRACT: Coatings consisting of polymer brushes are an effective way to modify solid interfaces. Polymer brush-modified hybrid particles have been prepared by surface-initiated activators regenerated by electron transfer atom transfer radical polymerization (SI-ARGET ATRP) of 2-(diethylamino)ethyl methacrylate (DEA) on silica particles. We have optimized the synthesis with respect to changing the reducing agent, temperature, and reaction solvent from an aqueous ethanol mixture to an aqueous methanol mixture. Our flexible electrostatically adsorbed macroinitiator approach allows for the modification of a variety of surfaces. Polybasic brushes have been grown on silica particles of different sizes, from 120 to 840 nm in diameter, as well as on wafers, and a comparison of the products has allowed the effect of surface curvature to be elucidated. An examination of the thickness of the dry brush and the aqueous hydrodynamic brush at both pH 7 and at 4 demonstrated that growth increased substantially with substrate curvature for particles with a diameter below 450 nm. This is attributed to the increasing separation between active chain ends, reducing the rate of termination. This is believed to be the first time that this effect has been demonstrated experimentally. Furthermore, we have seen that polymer brush growth on planar wafers was significantly reduced when the reaction mixture was stirred.

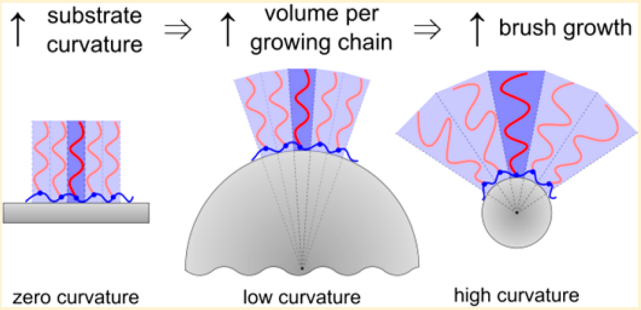

INTRODUCTION

Polymer brushes, formed by attaching one end of a polymer to an interface, display properties that can be attributed to both the free polymer and to the effects of chain confinement due to tethering at the interface. Surface properties can be tailored depending on the monomer used to form the brush, allowing control over the resulting interfacial hydrophilicity,[1] lubricity,[2] and response to external stimuli such as temperature or pH.[3] The modification of particulate interfaces can produce hybrid particles with dramatically different properties than those of the precursor materials. For example, the stability of particles in suspension may be significantly improved by adding a polymer brush to impart steric stability, making the suspension stable under a broad range of conditions.

Polymer brushes may be formed by reacting end-functional polymers with functionality on a surface using a "grafting to" approach; however, there are kinetic, steric, and entropic factors that limit the grafting density that can be achieved by this approach.[4,5] Surface-initiated polymerization (SIP) is a "grafting from" technique whereby the polymer is formed in situ from initiator sites that are immobilized on the surface, overcoming many of the limitations of the former approach.[6] Surface-initiated atom transfer radical polymerization (SI-ATRP) is widely used for SIP because of its controlled nature, the range of potential monomers, and the ability to use relatively mild reaction conditions. However, potential drawbacks of ATRP are that the copper(I) activator species is oxygen-sensitive and the optimum reaction conditions are often monomer-specific, requiring elucidation if truly controlled growth is desired.

Surfaces must be functionalized with initiator moieties before they can be used in SIP, and there are a range of techniques available to achieve this.[6−10] In this work we have employed a broadly applicable macroinitiator approach; specifically, we employed the electrostatic adsorption of a cationic copolymer containing the initiator functionality onto negatively charged silica substrates[11,12] that requires a single surface treatment, in contrast to the layer-by-layer macroinitiator approach.[13,14] Using a macroinitiator removes the requirement to synthesize halogen-containing silane species, which often require a stringently water-free step.[6] Our flexible approach also permits the modification of different surfaces, such as planar wafers and particles of different sizes, so that they have equivalent initiator-density because adsorption from solution readily permits uniform and complete coverage of the substrate with the initiator.

Received: January 30, 2013
Revised: April 23, 2013
Published: April 25, 2013

 © 2013 American Chemical Society dx.doi.org/10.1021/la4004092 | *Langmuir* 2013, 29, 6131−6140

Activators regenerated by electron transfer (ARGET) ATRP is a novel, recent variant of ATRP wherein a reducing agent generates the active, oxygen-sensitive Cu(I) catalyst species in situ by reduction of the oxidatively stable Cu(II) deactivator.[15,16] Because the reducing agent is present in excess, it imparts a degree of oxygen tolerance to the polymerization, hence requiring less stringently controlled conditions than conventional ATRP. In addition, the copper catalyst concentration can be decreased, even down to parts per million levels,[15,16] reducing the requirement for catalyst removal and making it a more industrially attractive technique.

We previously reported on the suitability of SI-ARGET ATRP for growing poly(2-(diethylamino)ethyl methacrylate) (poly(DEA)) brushes on 120 nm diameter silica particles[17], where we demonstrated their aqueous pH-responsive behavior. We have since expanded on that work by using a range of conditions to synthesize hybrid particles. In the first part of this Article, we report on the optimization of poly(DEA) brush growth kinetics on 120 nm particles when changing the reducing agent, temperature, and reaction solvent from an aqueous ethanol mixture to an aqueous methanol mixture. From these data, we are able to detail a more efficient synthesis methodology than we previously reported for SI-ARGET ATRP of poly(DEA) brushes generated from an electrostatically adsorbed macroinitiator.

In the second part of this study, we have investigated the effect of colloidal substrate curvature on polymer brush growth kinetics. The conformation of polymer brushes grown on flat substrates has been well studied following early work by Alexander[18] and de Gennes.[19] The volume available for chains to occupy linearly increases as the distance increases away from the planar interface, resulting in a linear dependence between the brush thickness and the chain length, assuming a constant grafting density. The conformation of polymer brushes at curved interfaces with fixed brush length has also been the topic of numerous theoretical studies,[20−22] and at high grafting densities, the conformational transitions from concentrated to semidilute polymer brush regimes have been identified.[23] Chen et al. have grown short brushes using various monomers on silica particles of 30 and 120 nm diameter that were functionalized with a cationic macroinitiator.[24] Moreover, Kotsuchibashi et al. recently reported the growth of short poly(DEA) brushes by SI-ATRP on 20 and 128 nm diameter silica particles.[25] However, in both of these studies the influence of surface curvature was not reported. We are specifically interested in determining whether the substrate curvature affects polymer brush *growth*, rather than the earlier, largely theoretical work that has looked at how curvature affects the conformation of solvated brushes of a given length or degree of polymerization.[20−22] We are undertaking this work to probe the impact that these geometric constraints impose when the chain end is an active polymerization site. Importantly, in further contrast to the existing theoretical work on brush conformation, we initially focus on the dry, fully collapsed brush in the absence of solvent to concentrate on the total amount of polymer that has been incorporated into the brush, before we look at their solution properties. We propose that brushes of greater thickness will be grown on smaller particles because of a lower rate of termination, as the increased curvature results in a greater distance between active sites. To test this hypothesis, we have synthesized poly(DEA) brushes on silica particles with diameters ranging from 120 to 840 nm and compared them to brush growth on planar wafer substrates.

EXPERIMENTAL SECTION

Materials. A range of sizes of AngstromSphere colloidal silica were supplied by Fiber Optic Center, and used as received. The manufacturer-quoted size and the actual particle diameters (measured by scanning electron microscopy (SEM) and hydrodynamic diameters measured by dynamic light scattering (DLS)) are reported in Table 1. In this Article, the silica particles will be referred to by their measured SEM diameter rounded to two significant figures.

Table 1. Details of the As-Received AngstromSphere Colloidal Silica Particles Used in This Study

silica sample name (nm)	manufacturer quoted diameter (μm)	SEM diameter (nm)	hydrodynamic diameter (DLS) (nm)
120	0.1	120 ± 7	124 ± 4
200	0.25	202 ± 11	236 ± 4
450	0.5	448 ± 14	486 ± 36
840	1.0	839 ± 18	957 ± 49

The inhibitor was removed from 2-(diethylamino)ethyl methacrylate monomer (DEA, Aldrich, 99%) using a short alumina column (activated, basic), and inhibitor-free monomer was stored at −20 °C and warmed to room temperature immediately before use. Copper(II) bromide (99.999%), 2,2′-bipyridine (≥99%), L-ascorbic acid (≥99%), and (+)-sodium L-ascorbate (≥98%) were purchased from Aldrich and used as received. Ethanol (absolute, Ajax Finechem) was distilled before use, and Milli-Q water was used throughout.

The cationic poly[2-(dimethylamino)ethyl methacrylate-*stat*-glycerol monomethacrylate] (PDMA-PGMA)-based water-soluble macroinitiator (MI), the structure of which is shown in Figure 1, was previously reported.[17] The $PDMA_{65}$-$PGMA_{29}$ statistical copolymer precursor (M_n = 14 880; M_w/M_n = 1.27) was confirmed to contain a molar ratio of 2:0.9 DMA/GMA units by ^{1}H NMR. The copolymer precursor was sequentially derivatized to produce the macroinitiator by esterifying the dihydroxy-functional glycerol residues with 2-bromoisobutyryl bromide to provide the ATRP initiator sites and then by quaternizing the tertiary amine groups with methyl iodide, making the copolymer water-soluble and cationic to promote adsorption on the negatively charged silica substrates.[7,24] The resulting macroinitiator contained approximately a 1:1 ratio of initiator to positively charged sites.

Macroinitiator Adsorption onto Silica Particles. The cationic macroinitiator was adsorbed onto the silica particles (2.0 g) by the dropwise addition of a well-dispersed 10 wt % aqueous suspension of silica to an equal volume of 4 mg/mL macroinitiator. The resulting 5 wt % silica, 2 mg/mL macroinitiator suspension was stirred overnight to allow the adsorption to reach equilibrium. The concentration of macroinitiator was high enough to achieve a maximum adsorbed amount on the silica, although not so high as to cause flocculation. Macroinitiator-modified silica particles were recovered by centrifugation, and washed by 2 cycles of redispersion in water and centrifugation.

Poly(DEA) Brush Growth on Particles by SI-ARGET ATRP. DEA monomer (20.00 g) was dissolved in an equal volume of solvent (typically 4:1 v/v ethanol (16 mL)/water (4 mL)), and the resulting mixture was divided in half. One half was used to disperse the macroinitiator-modified silica particles and the resulting suspension was deoxygenated by bubbling with nitrogen for 15 min. The second half was separately deoxygenated before copper (II) bromide ($CuBr_2$, 0.0096 g), 2,2′-bipyridine (bpy, 0.067 g), and sodium ascorbate (Na asc., 0.086 g) was added (DEA/$CuBr_2$/bpy/Na asc. molar ratio of 2500:1:10:10 were present in the final polymerization mixture). The polymerization was initiated by combining the macroinitiator-modified silica particle suspension with the reaction mixture in a separate deoxygenated 100 mL round-bottomed flask, and the resulting polymerization mixture contained ∼4 wt % silica. The polymerization was carried out under a positive pressure of nitrogen, typically at room temperature (∼22 °C), and samples were withdrawn at timed

dx.doi.org/10.1021/la4004092 | *Langmuir* 2013, 29, 6131−6140

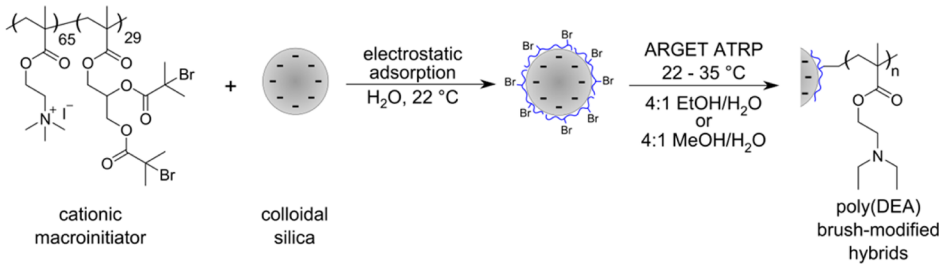

Figure 1. Reaction scheme depicting the electrostatic adsorption of the cationic macroinitiator onto colloidal silica particles and subsequent poly(DEA) brush growth by SI-ARGET ATRP.

intervals. Samples were diluted with cold (4 °C) 1:1 ethanol/water (oxygenated) to slow the reaction and were centrifuged to separate the poly(DEA)-brush particles from the reaction mixture, quenching the reaction. Brush-modified particles were further washed with 1:1 ethanol/water by successive redispersion and centrifugation cycles before analysis. For the hybrid particles that were synthesized to investigate the effect of surface curvature, the maximum monomer incorporation into the hybrid products corresponded to less than 14% monomer depletion for the synthesis of the 120 nm hybrids, <6% for the 200 nm hybrids, and <1% for both the 450 and 840 nm silica hybrids after 6 h of brush growth.

Silica Wafer Preparation and Macroinitiator Adsorption. Pieces of oxidized silicon wafer with a 2.5 nm oxidized silica layer (measured by ellipsometry) were irradiated for 20 min with UV/ozone (Bioforce UV/Ozone cleaner, ~9 mWcm^{-2} at 254 nm) before they were sonicated in Milli-Q water for 20 min. The wafers were rinsed with Milli-Q water, immersed in 10 wt % sodium hydroxide solution for 30 s, and then rinsed with copious amounts of Milli-Q water. The cleaned wafers were then immersed in a 1 mg/mL macroinitiator solution for 16 h to allow the adsorption to reach equilibrium. The macroinitiator-modified wafers were removed from the macroinitiator solution, rinsed with copious Milli-Q water, and blown dry under a stream of nitrogen before they were used in a brush growth reaction.

Poly(DEA) Brush Growth on Wafers by SI-ARGET ATRP. The reaction conditions and reagent ratios were the same as described above for particles. The macroinitiator-modified wafers were sealed in vials and deoxygenated by purging with nitrogen for 15 min. For reactions where the mixture was not stirred, the wafers were positioned diagonally in the vial with the oxidized, macroinitiator-adsorbed surface angled downward. For stirred reactions, the wafers were positioned on top of PTFE supports that allow free rotation of a small magnetic stirring bar beneath and hold the wafer at a similar angle to that of the wafers in unstirred reactions. DEA monomer (20.00 g) was dissolved in an equal volume of solvent (typically 4:1 (v/v) ethanol (16 mL)/water (4 mL)) and deoxygenated by purging with nitrogen for 15 min before copper(II) bromide ($CuBr_2$, 0.0096 g), 2,2′-bipyridine (bpy, 0.067 g), and sodium ascorbate (Na asc., 0.086 g) was added (DEA/$CuBr_2$/bpy/Na asc. molar ratio of 2500:1:10:10). The polymerization was started by adding a sufficient amount of dark brown-reaction mixture to immerse each of the wafers. The polymerization was carried out under a positive pressure of nitrogen at room temperature (~22 °C), and one vial was used for each growth time. Once the target growth time was reached, the brush-modified wafers were removed from the reaction mixture, washed by multiple sequential rinses of ethanol and then water, and blown dry under a stream of nitrogen before analysis.

Instrumentation. Solvent relaxation NMR experiments were performed to assess the macroinitiator adsorption on silica particles as measured through interfacial solvent displacement using the Acorn Area particle sizer from XiGo Nanotools.[26] The Carr–Purcell–Meiboom–Gill (CPMG) pulse sequence was used with a spacing between the 180° pulses of 1 ms (i.e., τ = 0.5 ms), and data were collected for 20 μs at the top of the even echoes. Spin–spin relaxation rates (R_2) were obtained by fitting a single exponential to the phase- and baseline-corrected signal. The relaxation data are reported as the specific relaxation rate enhancement, $R_{2sp} = (R_2/R_{2b}) - 1$, where R_{2b} is the experimentally determined relaxation rate of the bulk water.[27]

The infrared spectra were recorded on a PerkinElmer Spectrum Two FTIR spectrometer with a UATR Two attachment and were an average of four scans. The reported spectra were normalized to the SiO_2 peak at about 1100 cm^{-1}.[28] For SEM analysis, suspensions of hybrid particles were dried on silicon wafers, and no conductive coating was added before the images were obtained on a Zeiss VP FESEM. The images were obtained from 3 to 10 kV using either a secondary electron or InLens SE detector. Thermogravimetric analysis (TGA) was performed from 30 to 600 °C on a PerkinElmer Diamond TG/DTA thermal analyzer using aluminum pans and at a ramp rate of 10 °C/min under a constant flow of 30 mL/min nitrogen. Polymer weight percentage compositions were calculated using the mass loss from 150 to 500 °C (to ensure that the solvent was excluded) after subtracting the mass loss that was recorded for unmodified silica over this temperature range. The calculation of the geometric dry brush thickness used a measured density of 1.9 g/cm^3 for silica, and assumed a density of 1.1 g/cm^3 for the polymer.

The DLS and zeta potential measurements were recorded on a Malvern Instruments Zetasizer Nano-ZS. These measurements were made with 0.01 M KNO_3 background electrolyte, and the pH adjustments were performed using either HNO_3 or KOH and were accurate to ±0.1 pH unit. DLS measurements collected the backscattered intensity at 173°, and reported values are an average of at least 10 runs of 20 s each. The hydrodynamic brush thickness was calculated by subtracting the unmodified silica hydrodynamic diameter from the value obtained for the sample. The zeta potential measurements were an average of at least three measurements, each consisting of >20 runs. The errors reported for the DLS and zeta potential measurements are standard deviations.

The imaging ellipsometer measurements were performed on a Nanofilm EP3 Imaging Ellipsometer with a 523 nm wavelength laser using EP3View software to control the ellipsometer operation. The dry brush thickness values were modeled with WVASE32 software. The model consisted of a 1 mm (optically infinite) silicon layer, followed by a 2.5 nm silica layer (experimentally determined for the unmodified silicon wafer) and an uppermost poly(DEA) layer with a refractive index of n = 1.517.[29] The thickness of the polymer layer was the only unknown variable in the model.

RESULTS AND DISCUSSION

Macroinitiator Adsorption onto Silica Particles. The silica particles were functionalized with ATRP initiator sites through the physisorption of a cationic macroinitiator. The hydrodynamic diameters of the macroinitiator-modified silica were measured by DLS to be 126 ± 3, 237 ± 13, 482 ± 33, and 970 ± 42 nm for the four particle sizes investigated and are very close to those of the unmodified silica reported in Table 1. The adsorbed macroinitiator was estimated by TGA to be less than 1 wt % of the macroinitiator-modified silica for all of the particle sizes. For the 120 nm diameter particles, this is equivalent to a maximum surface excess of 0.4 mg/m^2 on the

dx.doi.org/10.1021/la4004092 | Langmuir 2013, 29, 6131–6140

basis of the silica particle SEM diameter and the measured density of 1.9 g/cm^3.

The adsorption isotherm for the macroinitiator adsorption on silica particles was not accessible by traditional depletion approaches. The UV spectra of the macroinitiator solutions are dominated by the iodide counterion, and it is unclear in what proportion the iodide anion adsorbs relative to the macroinitiator, information that is required for this technique to return meaningful data. In addition, the refractive indices of the macroinitiator solutions are close to that of water, making this technique similarly unsuitable. However, the pseudoisotherm for macroinitiator adsorption on silica was measured by solvent relaxation NMR for the smallest silica particle size (Figure 2).

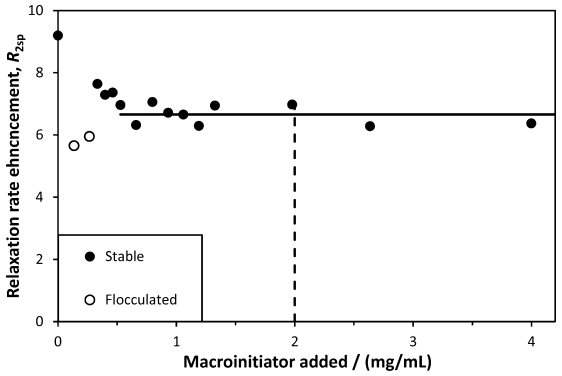

Figure 2. Specific relaxation rate enhancement (R_{2sp}) as a function of macroinitiator to particle ratio for 5.0 wt % dispersions of 120 nm diameter silica in water, showing a train layer saturation plateau above ~0.5 mg/mL of the added macroinitiator. The added concentration (2 mg/mL, dashed line) that was used when adsorbing the macroinitiator onto particles for subsequent polymer brush growth is well within the plateau region.

The addition of the macroinitiator caused a decrease in the specific relaxation rate enhancement, R_{2sp}. The adsorption of polymer to the silica surface gave a reduction in the relaxation rate because water is displaced from the silica surface by the adsorption of the macroinitiator, and the new macroinitiator-water interface has a lower specific surface relaxivity. Previous experiments with uncharged water-soluble polymers typically showed an increase in specific surface relaxivity upon adsorption of polymer as more water is bound to the silica surface.[27,30] However, Schwarz and Schönhoff reported a reduction in relaxation rates on addition of a polyelectrolyte to latex particles.[31] This was attributed to the replacement of surface-bound water with polymer train segments, which our data suggests is the dominant factor that influences relaxation rates upon adsorption of the macroinitiator on silica particles.

At low concentrations of the macroinitiator (<0.5 mg/mL), there is a larger degree of scatter in R_{2sp}, which is characteristic of a system of marginal colloidal stability. Moreover, at very low added macroinitiator concentrations (<0.3 mg/mL), incomplete surface coverage caused charge patch flocculation (open symbols in Figure 2). These samples measured lower relaxation rates because of the reduced surface area available.[26] We have previously shown that charge reversal occurs when this macroinitiator is adsorbed onto 120 nm silica particles from a 2 mg/mL solution.[17] The NMR data in Figure 2 are consistent with a transition, as more of the macroinitiator is added, from negatively charged silica, through marginally stable particles with a low net surface charge, to more stable, positively charged particles with a constant zeta potential of 34 ± 2 mV above 0.5 mg/mL of the added macroinitiator. The zeta potential of the macroinitiator-modified 200 nm silica was found to be within the error of the 120 nm silica.

A plateau in R_{2sp}, corresponding to the saturation of the macroinitiator train layer on the surface,[27,30] is observed for added macroinitiator concentrations above 0.5 mg/mL, as shown by the solid line in Figure 2. Above this concentration we can conclude that further addition of the macroinitiator to the bulk solution does not change the train layer of the adsorbed polymer because the solvent relaxation rate is sensitive only to the bound solvent close to the interface.[27,30] The difference between the train layer saturation concentration and the maximum adsorbed amount depends on the polymer and surface used, and was explored in detail by Cattoz et al. for a weakly adsorbing polymer on silica.[30] For our strongly adsorbing cationic macroinitiator, it is reasonable to conclude that the difference between these two concentrations is minimal and that 0.5 mg/mL gives a saturated surface coverage. If all of the added macroinitiator were to adsorb, 0.5 mg/mL would correspond to an adsorbed amount of ~0.4 mg/m^2. This is in agreement with the maximum adsorbed amount estimated by TGA above.

The pseudoisotherm was only studied in detail for the smallest particle size (120 nm diameter); however, for the larger particle sizes, sufficient solvent relaxation samples were measured to verify that the macroinitiator concentrations used for the subsequent polymerizations were also in the train layer saturation plateau. Furthermore, the particle mass fraction and added macroinitiator concentration were kept constant at 2 mg/mL for all subsequent polymerizations, corresponding to higher added macroinitiator to surface area ratios for the larger particles. We conclude, therefore, that we are working with a maximum and reproducible initiator site density across all particle sizes.

Poly(DEA) Brush Growth on Particles. Poly(DEA) brush growth from the macroinitiator-modified silica was confirmed by inspecting the infrared spectra of the resulting hybrid materials. Spectra of the hybrid materials, such as shown in Figure 3 for hybrids based on 120 nm silica particles, show an increasing poly(DEA) contribution with increasing growth time. This was confirmed by the increasing intensity of C−N, C═O, and C−H absorbance at 1400, 1730, and 2980 cm^{-1},

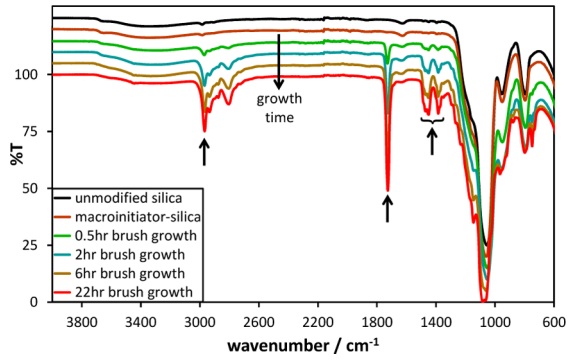

Figure 3. Infrared spectra of the unmodified silica, the macroinitiator-modified silica, and the poly(DEA) brush-modified silica particles showing the evolution of peaks from the poly(DEA) brush as a function of polymerization time. Data have been vertically offset for clarity. Reaction conditions: 4:1 ethanol/water, sodium ascorbate reducing agent, room temperature (~22 °C).

dx.doi.org/10.1021/la4004092 | Langmuir 2013, 29, 6131−6140

respectively, which is not present in the spectra of either the unmodified or the macroinitiator-modified silica.

Although IR demonstrated the presence of increasing poly(DEA) content with increasing growth time, these data do not quantify the brush content of the hybrids. Therefore, brush growth was quantified by measuring the weight percentage polymer composition of the hybrid by TGA. This value allowed for the calculation of a geometric dry brush thickness, t, using eq 1 (derivation in Supporting Information). The dry brush thickness is the radius of an idealized core−shell hybrid particle and corresponds to the measured weight percentage of the polymer content minus the radius of the unmodified silica core

$$t = r\left[\sqrt[3]{\frac{\phi(\rho_p - \rho_b) + \rho_p}{\rho_b(1-\phi)}} - 1\right] \quad (1)$$

where r is the silica particle radius, ϕ is the polymer mass fraction, and ρ_p and ρ_b are the densities of the particle and polymer brush, respectively.

Effect of Alcohol Solvent. We have successfully grown poly(DEA) brushes on 120 nm diameter silica particles in both aqueous ethanol and aqueous methanol solvents (constant 4:1 volume ratio of alcohol/water). In both syntheses, ascorbic acid was the reducing agent and the temperature was 35 °C. As shown in Figure 4, hybrid particles that were grown in aqueous

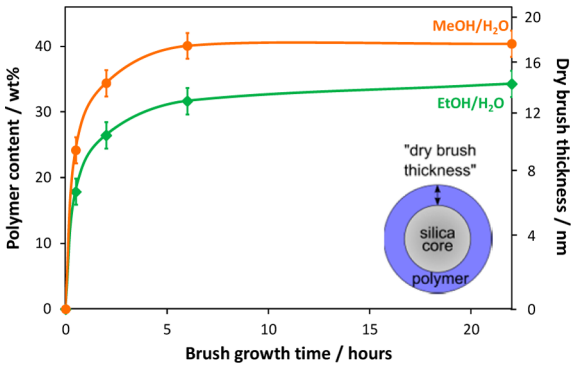

Figure 4. Evolution of the polymer content determined by TGA and the derived dry brush thickness of poly(DEA) brush-modified 120 nm silica particles using either aqueous ethanol or aqueous methanol as the solvent. Reaction conditions: 4:1 alcohol/water, ascorbic acid reducing agent, temperature 35 °C. Please note that the dry brush thickness is calculated from the polymer weight percent according to eq 1, but this is not a linear function. Thus the secondary y-axis is not linear.

methanol had a higher polymer content, equivalent to a greater dry brush thickness, than hybrid particles that were synthesized in aqueous ethanol for an equivalent growth time. SI-ARGET ATRP is expected to respond to changes in the synthesis conditions in much the same way as does conventional ATRP, where increased solvent polarity increases the rate of polymerization.[32] However, in ARGET ATRP the equilibrium between the copper and the reducing agent is an additional consideration, so that if subtle changes in the reaction conditions change this equilibrium then the resulting change in activator (Cu(I)) to deactivator (Cu(II)) ratio would affect the kinetics accordingly. As the polymerization rate increased in line with the conventional ATRP expectation resulting from the increased polarity of methanol compared to that of ethanol, it is reasonable to conclude that the equilibrium between the copper and the reducing agent was relatively unaffected by the change in alcohol.

As observed previously,[17] brush growth proceeds rapidly in the early stages of polymerization in both solvents, but the rate of brush growth decreases over longer time scales. This nonlinear kinetic profile is often indicative of a loss of control of the polymerization, possibly due to chain termination and/or catalyst deactivation.[33] However, because the brushes are being grown from curved particulate interfaces, the kinetic profile of perfectly living brush growth would not display a linear increase in polymer content with time. Instead, the kinetic plot is expected to be curved because of the increasing volume that is available for chains to occupy as the distance from the particulate substrate surface increases. Chains that are grown from a curved interface effectively occupy a truncated, cone-shaped region, whereas chains that are grown on a planar substrate occupy a regular prism extending normal from the interface. Equation 2 describes how the polymer brush layer thickness, t, on a curved substrate, radius r, is expected to relate to the thickness of the same brush layer on a planar substrate, t_p.

$$t = r\left[\sqrt[3]{\frac{3t_p}{r} + 1} - 1\right] \quad (2)$$

Figure S1 in the Supporting Information presents some examples of this scaling relationship for a selection of particle sizes, illustrating the effect of surface curvature on the kinetic profiles of brush growth on particles.

The kinetic profiles in Figure 4, however, show limited growth over time scales greater than 6 h, and the curtailment of growth is more marked than would be expected solely on the basis of the impact of surface curvature. Therefore, it is likely that either chain termination or catalyst deactivation has had an impact on the polymer brush growth over these longer growth times. Since there was little difference in the degree of apparent control of the polymerization between the two aqueous alcohol solvents, ethanol was chosen for further study despite producing thinner brushes than those produced in aqueous methanol for equivalent amounts of time. This is because a slower polymerization rate should also decrease the rate of side reactions; furthermore, ethanol is cheaper and more environmentally benign, increasing its industrial relevance.

The kinetics of poly(DEA) brush growth were less sensitive to slight changes in reaction temperature (Figure S2). As is generally expected for ATRP,[32] the lower temperature slightly slowed the initial rate and allowed the brush to continue growing to a greater thickness over longer reaction times, so the reduced temperature was used for later syntheses. While we investigated the effect of temperature, the importance of keeping the reaction mixture free-flowing was highlighted and is further discussed in the Supporting Information.

Effect of Reducing Agent. The advantage of using ARGET ATRP over conventional ATRP is the use of a reducing agent, which imparts a degree of oxygen tolerance to the polymerization reaction. Figure 5 shows the impact of two reducing agents on the SI-ARGET ATRP of poly(DEA) on 120 nm silica particles. Thicker brushes were grown when sodium ascorbate was used as the reducing agent than when ascorbic acid was used. UV studies have shown that sodium ascorbate is more efficient at reducing Cu(II) to Cu(I) than ascorbic acid (Figure S3), so the difference may be due to subtle changes in

dx.doi.org/10.1021/la4004092 | Langmuir 2013, 29, 6131−6140

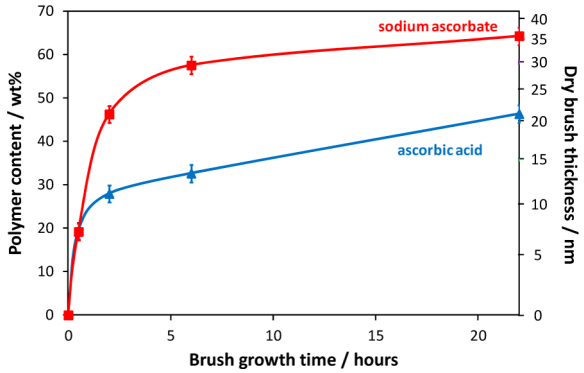

Figure 5. Kinetic profiles showing the effect of changing the reducing agent from ascorbic acid to sodium ascorbate on the evolution of the TGA polymer content and dry brush thickness of poly(DEA) brush-modified 120 nm diameter silica particles. Reaction conditions: 4:1 ethanol/water, room temperature (~22 °C). Please note that the secondary *y*-axis is not linear; see eq 1.

the copper catalyst concentration. Previous studies have shown that different reducing agents offer different activities and control when they are used in ARGET ATRP,[34] though the precise nature of their influence remains unclear.

Brush Growth on Planar Surfaces. Poly(DEA) brushes have also been grown on macroinitiator-modified planar oxidized silicon wafers. Not stirring the reaction mixture is a common practice when brushes are grown on the wafers.[33,35,36] However, it was our intention to compare the brush growth under similar conditions between those used for wafers and those used on curved particulate substrates, which have to be stirred to stop the particles from settling. To quantify the effect of stirring on brush growth on wafers, we conducted syntheses with and without stirring. Figure 6 compares the resulting brush

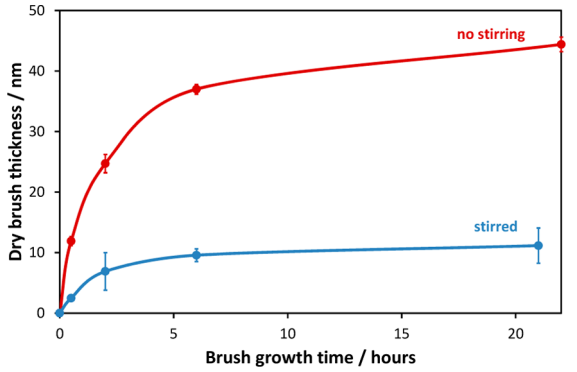

Figure 6. Ellipsometric dry brush thickness as a function of growth time for poly(DEA) brushes grown from macroinitiator-modified planar oxidized silicon wafers, showing the effect of stirring the reaction mixture. Each data point represents a separate wafer. Each reported value is an average of three measurements, each taken at a separate spot on the wafer surface, and the error bars represent the standard deviation. Reaction conditions: 4:1 ethanol/water, sodium ascorbate reducing agent, room temperature (~22 °C).

growth kinetics and clearly shows that for all of the growth times stirring the reaction mixture dramatically decreased the thickness of the grown polymer layer.

Stirring was expected to have two effects on the polymerization: increasing the resupply of reagents that have become depleted in the vicinity of the surface, such as the monomer or reducing agent, and increasing chain motion, which may decrease the rate of polymerization by increasing the rate of termination by the radical combination of neighboring chains. Our results clearly indicate that the rate of polymerization decreases with stirring, which is attributed to a combination of increased termination reactions and to different reagent concentrations in the vicinity of the growing chain ends, as complementary experiments have shown no indication of either macroinitiator or brush desorption in a good solvent for the brush. Our observations are in agreement with previous studies that have shown that stirring decreases the thickness of brushes grown by ATRP on planar substrates;[36] however, our decrease in brush growth of approximately 75% is of greater magnitude than the previously reported 50% reduction, which can be attributed to differences in the experimental configuration.

In addition to the decreased brush thickness, the brushes that were grown under stirred conditions were less uniform across the wafer than those that were grown in the absence of stirring, as shown by their greater error bars in Figure 6. This is presumably due to the increased termination reactions occurring at various locations across the wafers (perhaps due to local differences in turbulence and mixing) and is an interesting juxtaposition against the intuitive argument that stirring would increase the homogeneity by ensuring good mixing. Overall, the decrease in brush growth may be attributed to increased termination due to increased chain dynamics, and the data suggests that this is the dominant factor that outweighs any potential increase in growth due to both better mixing and the supply of reagents. For the purposes of this study, the stirred series will be used to compare to the growth on curved particulate substrates in the following section. However, if one wishes to achieve the best brush growth on wafers, an unstirred approach is recommended.

Effect of Surface Curvature. It is reasonable to propose that the positively charged macroinitiator used in this study adsorbs with equivalent surface excess to all of the silica substrates used because the zeta potential measurements showed that the unmodified silica particles each have the same surface charge density, and the 120 and 200 nm macroinitiator-modified silica have the same surface charge density. Moreover, the solvent relaxation NMR experiments (Figure 2) confirm that the concentration of macroinitiator used when adsorbing to the silica particles (2 mg/mL) was within the plateau surface excess concentration for each particle size. This maximum surface excess was confirmed to be ~0.4 mg/m^2 by TGA measurement of the 120 nm silica particles. For the larger particle sizes, however, the macroinitiator adsorption cannot be quantified by TGA because of the low polymer mass fraction. From the combination of these three measurements, we conclude that our macroinitiator approach allows us to modify a range of silica surfaces of varying curvature with equivalent initiator densities.

From planar substrates, the volume available for chains to occupy increases linearly with distance from the surface, resulting in a linear dependence between the brush thickness and the chain length, assuming a constant grafting density. Spherical substrates, however, inherently provide a greater volume for chains to occupy as the distance from the surface increases. This increase in volume is amplified by the curvature of the interface which is defined as the inverse of the radius. These differences are illustrated schematically in Figure 7, calculated with eq 2, and shown in Figure S1.

The hypothesis we wished to investigate was whether increasing surface curvature would enhance brush growth

dx.doi.org/10.1021/la4004092 | *Langmuir* 2013, 29, 6131−6140

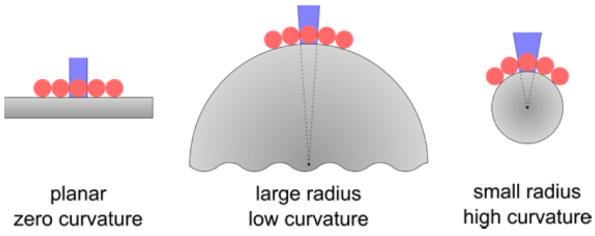

Figure 7. Schematic diagram illustrating how increasing the surface curvature increases the volume available for the chains to occupy (blue region) as the distance from the interface increases, where each solid red circle represents an initiator site.

under equivalent conditions because increasing curvature increases the average distance between growing chain ends, a topic that has been largely ignored to date. The theoretical spacing between two well-solvated rigid brush chains has been calculated geometrically, and is displayed in Figure S4. It is clear that as the particle size is reduced, the distance between the growing ends of the brush chains increases. This, in conjunction with the increased conformational entropy of brushes grown on smaller particles, may be expected to reduce the rate of interchain termination reactions.

We conducted a series of syntheses of poly(DEA) brushes on silica particles with diameters ranging from 120 to 840 nm. The weight fraction of the particles was kept constant in all syntheses, which means that the total interfacial surface area in the synthesis decreases as the particle size increases. Because the concentration of monomer in the initial solution was constant in all syntheses and the fact that we assumed a constant macroinitiator surface excess, the monomer to initiator site ratio was greater when larger particles were used. However, in all cases, the monomer was present in a large excess and its concentration may be effectively considered to be constant, meaning that the ATRP rate should not be affected by monomer consumption over the course of the brush growth. Figure 8a shows the dry brush thickness of poly(DEA) grown on different core silica sizes as a function of reaction time. In addition, the thickness of poly(DEA) brushes grown on wafers under stirred conditions have been added for comparison. We have concentrated on growth times of up to 6 h because, as was observed in Figures 4–6, growth is limited over longer time scales, and this Figure allows the trend over shorter growth times to be seen clearly.

Figure 8a shows a distinct trend toward increased dry brush thickness with decreasing particle size, that is, with increasing surface curvature. The brushes grown on the zero-curvature wafers under stirred conditions were the thinnest brushes for each growth time. Brush growth on particles was relatively independent of the particle size for the first 30 min of growth but diverged upon longer growth time. The brush growth rate rapidly decreased for the largest two particle sizes studied (450 and 840 nm), whereas brushes grown on the smallest particles (120 and 200 nm) displayed substantial continued growth over 5 to 6 h.

However, even if the rate of polymer growth was the same irrespective of particle size, the profiles for the dry brush thickness presented in Figure 8a would not be expected to overlap because of the increased volume that is available for chains to occupy on substrates with greater curvature. To remove the effect of surface curvature from the data, it is appropriate to consider an alternative measure, such as t_p, the dry thickness of an equivalent brush grown on a planar substrate (eq 2), which is proportional to the molecular weight of the brush arms. These profiles, shown in Figure 8b, would overlap if the rate of the polymer brush growth was independent of the surface curvature.

It is clear to see that Figure 8b emphasizes the trend observed in Figure 8a. The brush growth on wafers recorded the lowest values and is similar to growth on larger particles (450 and 840 nm diameter). These brushes that were grown on the substrates with the lowest curvature are comparable to one another, indicating that substrate curvature has little effect on the brush growth for particle diameters above 450 nm. The magnitude of brush growth on 200 nm diameter particles is significantly larger, but the largest values were obtained for brushes grown on 120 nm silica particles. This supports our original hypothesis and indicates that the increasing distance between neighboring chain ends that occurs with the increasing curvature shown in Figure S4 has a genuine effect on brush growth, resulting in reduced termination and increased brush growth on the smaller particles. This effect is substantial below a particle diameter of 450 nm. As far as we are aware, this is the first report of this effect.

Figure 9 shows the data that were presented in Figure 8b plotted against the silica core particle curvature, with the data grouped by growth times. If the polymer brush growth were independent of surface curvature, the trendlines fitted to the data would be horizontal, which is clearly not the case. The

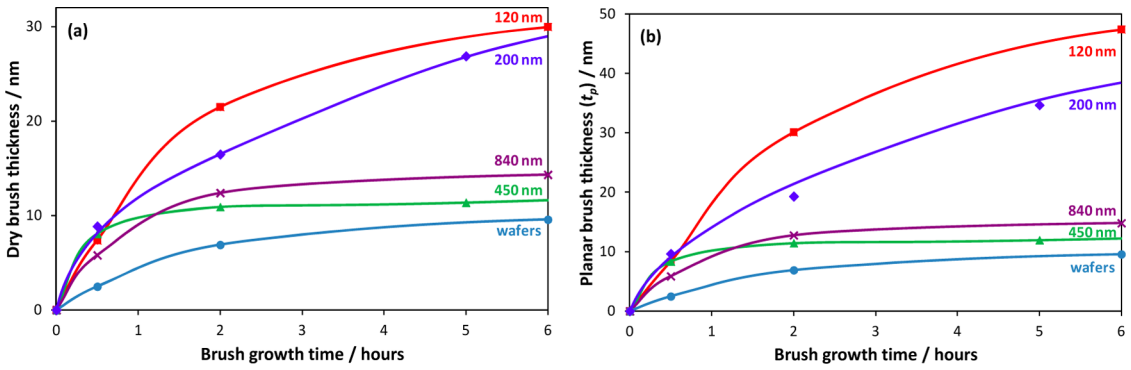

Figure 8. (a) Dry brush thickness and (b) equivalent thickness of the same brush layer on a planar substrate (t_p) calculated with eq 2 for brushes grown on wafers or particles of different sizes. The particle data is derived from TGA, and the wafer values are from ellipsometry measurements. All reactions were stirred. Reaction conditions: 4:1 ethanol/water, sodium ascorbate reducing agent, room temperature (~22 °C).

dx.doi.org/10.1021/la4004092 | *Langmuir* 2013, 29, 6131–6140

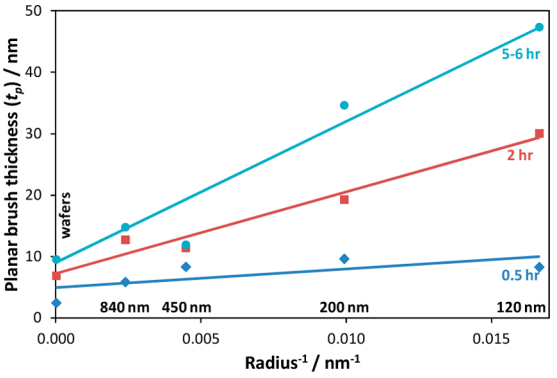

Figure 9. Equivalent brush thickness on a planar substrate (t_p), grouped by growth time and plotted against reciprocal silica particle radius.

increasing gradient of the trendlines indicates that there is a more pronounced effect of surface curvature with increasing growth time. Our data are consistent with a transition to a strong influence of substrate curvature on polymer growth as the substrate size decreases. The lower bound of this curvature effect is a curvature of 0.005 nm^{-1}. The identification of the relevant size range over which the substrate curvature becomes significant will aid the optimization of future polymer brush syntheses on curved substrates.

Hydrodynamic Brush Thickness. The hydrodynamic brush thickness of the poly(DEA) brushes grown on the 120, 200, and 450 nm silica particles, measured at pH 7, is given in Figure 10a. Data is not presented for the hybrids based on the 850 nm silica because these particles settled too rapidly for meaningful DLS measurement. In comparison to the dry brush thickness values measured by TGA in Figure 8a, the hydrodynamic brush thickness values are larger by a factor of at least 3 for all hybrids. Clearly, the poly(DEA) brushes that were immersed in aqueous electrolyte at pH 7 contain significant amounts of solvent, which is understandable given that free poly(DEA) has a pK_a of 7.3,[37] so more than half of the tertiary amine residues are protonated at pH 7. It is observed that, in contrast to the dry TGA data shown in Figure 8a, at pH 7 the hydrodynamic thickness of poly(DEA) brushes grown on 200 nm silica is greater than that of those grown on 120 nm silica. As stated above, the volume available for each chain is greater in the case of brushes grown on 120 nm particles than that of those grown on 200 nm particles; thus, the chains more readily adopt a coiled conformation on the smaller particles. Conversely, the chains on the 200 nm particles must adopt a comparatively more stretched conformation and as a result are measured to have a greater hydrodynamic thickness. In the case of the brushes grown on the 450 nm particles, the significantly reduced polymer content measured by TGA, combined with the lowest hydrodynamic thickness, indicates that these brushes have considerably lower degrees of polymerization.

The hydrodynamic thickness of these poly(DEA) brushes was also measured at pH 4 (Figure 10c). Under these conditions, the tertiary amine residues on the brushes become protonated, and each chain becomes highly positively charged. As such, there is significant intra- and interchain electrosteric repulsion, and the chains adopt an extended conformation to minimize these repulsive interactions. Additionally, there is significant additional ingress of solvent into the brush. A comparison of the data in Figure 10 clearly shows this phenomenon, as the hydrodynamic brush thickness is greater at pH 4 than at pH 7 for each polymer hybrid sample. Furthermore, the hybrid particles continue to demonstrate this conformational change over multiple cycles of pH change.[17] That is to say, the increased steric crowding within

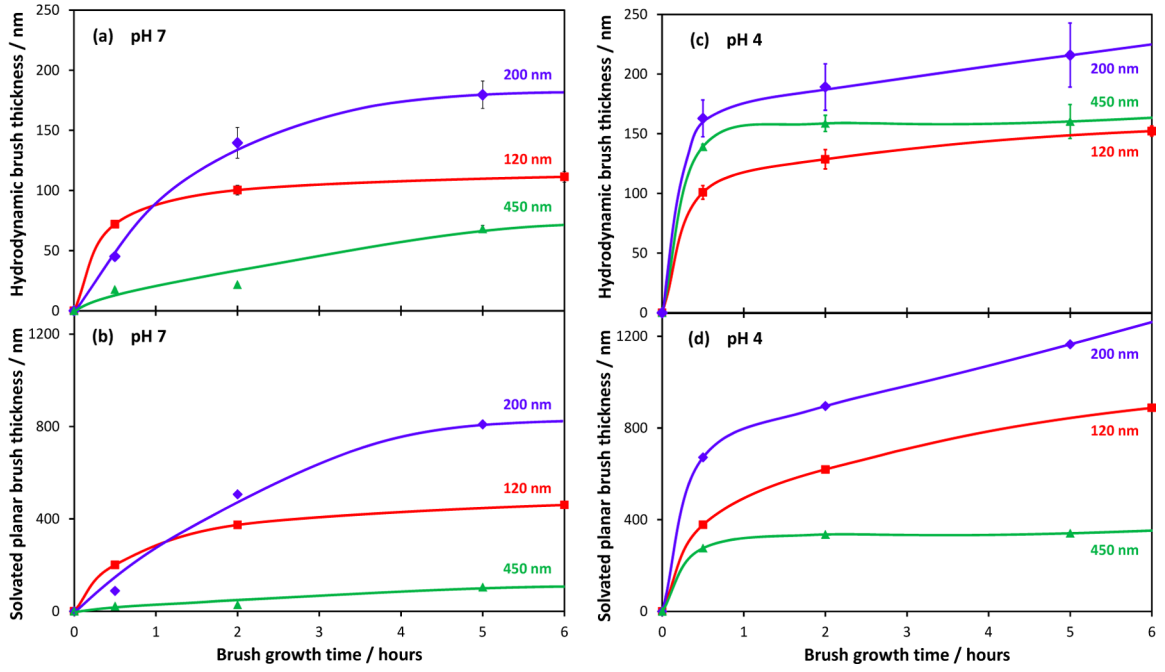

Figure 10. Hydrodynamic brush thickness (a and c) calculated from the hybrid hydrodynamic diameter and equivalent thickness of the same hydrated brush layer on a planar substrate (b and d) for brushes grown on 120, 200, and 450 nm diameter core silica particles in pH 7 (a and b) or pH 4 (c and d) aqueous solutions. Please note that lines are guides to the eye. The hybrids with 840 nm diameter core silica particles could not be accurately measured by DLS because of rapid settling.

dx.doi.org/10.1021/la4004092 | *Langmuir* 2013, 29, 6131−6140

the brush due to the swelling does not result in the detachment of brush chains.

When expressed as an equivalent solvated planar brush thickness, Figure 10b,d, it is clear that the hydrodynamic brush thickness values at both pH 7 and 4 are distinctly different for each particle size. Recall that this analysis is proportional to the molecular weight of the brush arms and would be equivalent if the surface curvature did not influence the data; clearly this is not the case. Indeed, upon comparing the equivalent dry planar brush (Figure 8b) and solvated planar brush (Figure 10b,d) thickness values it is apparent that the relative magnitude of the brushes grown on the 120 and 200 nm particles has reversed. The data clearly shows that the curvature of the substrate impacts both the polymerization (Figure 8b) and the solvated conformation (Figure 10b,d) of the brush.

The data in Figure 10c indicates that at pH 4 the hydrodynamic thickness of the brushes on 450 nm particles is greater than that of those on 120 nm particles. This is attributed to a combination of two effects. The dry TGA data shown in Figure 8 for brushes that were grown on 450 nm particles indicate significant chain termination. As a consequence, there is a decreased number of active chains per unit surface area as the growth time continues, and these active chains each have a relatively larger volume per chain. As discussed previously, this may allow the chains to grow longer because of decreased steric crowding. Recall that the TGA measurements average the polymer content over the entire particle and cannot resolve the degree of dispersity in the brush chains. However, it is well known that DLS measurements of brushes are influenced by relatively few longer chains; the technique detects all of the solvent that moves with the particle. This effect is magnified when the chains are fully extended, such as at pH 4 in the case of poly(DEA). The observed dramatic increase in hydrodynamic thickness of the poly(DEA) brushes on 450 nm particles when the solution is changed from pH 7 to 4 is therefore attributed to the dispersity in the brush, with a small number of longer chains trapping significant amounts of solvent.

CONCLUSIONS

We have used SI-ARGET ATRP to grow poly(DEA) brushes from an electrostatically adsorbed macroinitiator, and we report an optimized synthesis on 120 nm diameter silica particles with respect to changing the reaction temperature, reducing agent, and aqueous alcohol solvent. The polybasic brushes were seen to entrain a significant amount of solvent when in aqueous solution close to their pK_a, with additional solvent uptake upon exposure to acidic solution. Poly(DEA) brushes have also been grown from planar substrates, and the rate of brush growth was seen to be greatly reduced by stirring the reaction mixture. This reduction in rate may be due to increased chain motion, resulting in an increase in the rate of termination by radical combination.

We have shown that the rate of surface-initiated polymer brush growth depends on the curvature of the interface, with growth increasing significantly with curvature for particle diameters below 450 nm. This is due to the substrate curvature resulting in a greater separation between active chain ends, which decreases the rate of termination. We believe this to be the first experimental investigation into this effect. These findings will be of broad interest to anyone conducting surface-initiated polymerization because they demonstrate that polymerizations conducted under the same reaction conditions with the same reaction time do not produce equivalent brushes; rather, they are dependent on the substrate geometry.

ASSOCIATED CONTENT

Supporting Information

Derivation of equations, UV−vis spectra of Cu(I)/Cu(II) stock solutions and Cu(II) plus reducing agents, and kinetic profiles showing the effect of temperature on poly(DEA) brush growth. This material is available free of charge via the Internet at http://pubs.acs.org.

AUTHOR INFORMATION

Corresponding Author

*E-mail: erica.wanless@newcastle.edu.au.

Notes

The authors declare no competing financial interest.

ACKNOWLEDGMENTS

We thank the Australian Research Council for DP110100041. Y. Li and S. P. Armes are thanked for the synthesis and donation of the cationic macroinitiator, T. Murdoch is thanked for help with ellipsometry, and Y. Nakamura is thanked for useful discussions. S. Prescott is thanked for help with solvent relaxation NMR, and V. Coleman at the National Measurement Institute (Sydney, Australia) is thanked for facilitating access to the Acorn Area spectrometer.

REFERENCES

(1) Motornov, M.; Minko, S.; Eichhorn, K.-J.; Nitschke, M.; Simon, F.; Stamm, M. Reversible Tuning of Wetting Behavior of Polymer Surface with Responsive Polymer Brushes. *Langmuir* **2003**, *19*, 8077−8085.

(2) Klein, J. Shear Friction, and Lubrication Forces Between Polymer-Bearing Surfaces. *Annu. Rev. Mater. Sci.* **1996**, *26*, 581−612.

(3) Cohen Stuart, M. A.; Huck, W. T. S.; Genzer, J.; Muller, M.; Ober, C.; Stamm, M.; Sukhorukov, G. B.; Szleifer, I.; Tsukruk, V. V.; Urban, M.; Winnik, F.; Zauscher, S.; Luzinov, I.; Minko, S. Emerging Applications of Stimuli-Responsive Polymer Materials. *Nat. Mater.* **2010**, *9*, 101−113.

(4) Rühe, J.; Knoll, W. Functional Polymer Brushes. *J. Macromol. Sci., Part C: Polym. Rev.* **2002**, *42*, 91−138.

(5) Minko, S. Grafting on Solid Surfaces: "Grafting to" and "Grafting from" Methods. In *Polymer Surfaces and Interfaces, Characterization, Modification and Applications*; Stamm, M., Ed.; Springer: Berlin, 2008; pp 215−234.

(6) Edmondson, S.; Armes, S. P. Synthesis of Surface-Initiated Polymer Brushes Using Macro-Initiators. *Polym. Int.* **2009**, *58*, 307−316.

(7) Fielding, L. A.; Edmondson, S.; Armes, S. P. Synthesis of pH-Responsive Tertiary Amine Methacrylate Polymer Brushes and Their Response to Acidic Vapour. *J. Mater. Chem.* **2011**, *21*, 11773−11780.

(8) Fulghum, T. M.; Patton, D. L.; Advincula, R. C. Fuzzy Ternary Particle Systems by Surface-Initiated Atom Transfer Radical Polymerization from Layer-by-Layer Colloidal Core-Shell Macroinitiator Particles. *Langmuir* **2006**, *22*, 8397−8402.

(9) von Werne, T.; Patten, T. E. Atom Transfer Radical Polymerization from Nanoparticles: A Tool for the Preparation of Well-Defined Hybrid Nanostructures and for Understanding the Chemistry of Controlled/"Living" Radical Polymerizations from Surfaces. *J. Am. Chem. Soc.* **2001**, *123*, 7497−7505.

(10) Bain, E. D.; Dawes, K.; Özçam, A. E.; Hu, X.; Gorman, C. B.; Šrogl, J.; Genzer, J. Surface-Initiated Polymerization by Means of Novel, Stable, Non-Ester-Based Radical Initiator. *Macromolecules* **2012**, *45*, 3802−3815.

(11) Chen, X.; Armes, S. Surface Polymerization of Hydrophilic Methacrylates from Ultrafine Silica Sols in Protic Media at Ambient

Temperature: A Novel Approach to Surface Functionalization Using a Polyelectrolytic Macroinitiator. *Adv. Mater.* **2003**, *15*, 1558−1562.
(12) Liu, R.; De Leonardis, P.; Tirelli, N.; Saunders, B. Thermally-Responsive Surfaces Comprising Grafted Poly(N-isopropylacrylamide) Chains: Surface Characterisation and Reversible Capture of Dispersed Polymer Particles. *J. Colloid Interface Sci.* **2009**, *340*, 166−175.
(13) Wischerhoff, E.; Glatzel, S.; Uhlig, K.; Lankenau, A.; Lutz, J.-F.; Laschewsky, A. Tuning the Thickness of Polymer Brushes Grafted from Nonlinearly Growing Multilayer Assemblies. *Langmuir* **2009**, *25*, 5949−5956.
(14) Estillore, N. C.; Advincula, R. C. Free-Standing Films of Semifluorinated Block Copolymer Brushes from Layer-by-Layer Polyelectrolyte Macroinitiators. *Macromol. Chem. Phys.* **2011**, *212*, 1552−1566.
(15) Jakubowski, W.; Matyjaszewski, K. Activators Regenerated by Electron Transfer for Atom-Transfer Radical Polymerization of (Meth)acrylates and Related Block Copolymers. *Angew. Chem., Int. Ed.* **2006**, *45*, 4482−4486.
(16) Matyjaszewski, K.; Dong, H.; Jakubowski, W.; Pietrasik, J.; Kusumo, A. Grafting from Surfaces for "Everyone": ARGET ATRP in the Presence of Air. *Langmuir* **2007**, *23*, 4528−4531.
(17) Cheesman, B. T.; Willott, J. D.; Webber, G. B.; Edmondson, S.; Wanless, E. J. pH-Responsive Brush-Modified Silica Hybrids Synthesized by Surface-Initiated ARGET ATRP. *ACS Macro Lett.* **2012**, *1*, 1161−1165.
(18) Alexander, S. Adsorption of Chain Molecules with a Polar Head a Scaling Description. *J. Phys. (Paris)* **1977**, *38*, 983−987.
(19) de Gennes, P. G. Conformations of Polymers Attached to an Interface. *Macromolecules* **1980**, *13*, 1069−1075.
(20) Wijmans, C. M.; Zhulina, E. B. Polymer Brushes at Curved Surfaces. *Macromolecules* **1993**, *26*, 7214−7224.
(21) Zhulina, E. B.; Borisov, O. V. Polyelectrolytes Grafted to Curved Surfaces. *Macromolecules* **1996**, *29*, 2618−2626.
(22) Tagliazucchi, M.; Szleifer, I. Stimuli-Responsive Polymers Grafted to Nanopores and Other Nano-Curved Surfaces: Structure, Chemical Equilibrium and Transport. *Soft Matter* **2012**, *8*, 7292−7305.
(23) Dukes, D.; Li, Y.; Lewis, S.; Benicewicz, B.; Schadler, L.; Kumar, S. K. Conformational Transitions of Spherical Polymer Brushes: Synthesis, Characterization, and Theory. *Macromolecules* **2010**, *43*, 1564−1570.
(24) Chen, X. Y.; Armes, S. P.; Greaves, S. J.; Watts, J. F. Synthesis of Hydrophilic Polymer-Grafted Ultrafine Inorganic Oxide Particles in Protic Media at Ambient Temperature via Atom Transfer Radical Polymerization: Use of an Electrostatically Adsorbed Polyelectrolytic Macroinitiator. *Langmuir* **2004**, *20*, 587−595.
(25) Kotsuchibashi, Y.; Faghihnejad, A.; Zeng, H.; Narain, R. Construction of 'Smart' Surfaces with Polymer Functionalized Silica Nanoparticles. *Polym. Chem.* **2013**, *4*, 1038−1047.
(26) Fairhurst, D.; Prescott, S. W. The use of Nuclear Magnetic Resonance as an Analytical Tool in the Characterisation of Dispersion Behaviour. *Spectrosc. Eur.* **2011**, *23*, 13−16.
(27) Van der Beek, G. P.; Stuart, M. A. C.; Cosgrove, T. Polymer Adsorption and Desorption Studies via Proton NMR Relaxation of the Solvent. *Langmuir* **1991**, *7*, 327−334.
(28) Launer, P. J. Infrared Analysis of Organosilicon Compounds: Spectra-Structure Correlations. In *Silicon Compounds Register and Review*; Arkles, B., Ed.; Petrarch Systems, Inc: Bristol, PA, 1987; pp 100-103.
(29) Brandrup, J., Immergut, E. H., Grulke, E. A., Abe, A., Bloch, D. R., Eds.; *Polymer Handbook*, 4th ed.; John Wiley & Sons: New York, 2005.
(30) Cattoz, B.; Cosgrove, T.; Crossman, M.; Prescott, S. W. Surfactant-Mediated Desorption of Polymer from the Nanoparticle Interface. *Langmuir* **2012**, *28*, 2485−2492.
(31) Schwarz, B.; Schönhoff, M. A ^{1}H NMR Relaxation Study of Hydration Water in Polyelectrolyte Mono and Multilayers Adsorbed to Colloidal Particles. *Colloids Surf., A* **2002**, *198−200*, 293−304.
(32) Matyjaszewski, K. Atom Transfer Radical Polymerization (ATRP): Current Status and Future Perspectives. *Macromolecules* **2012**, *45*, 4015−4039.
(33) Matyjaszewski, K.; Miller, P. J.; Shukla, N.; Immaraporn, B.; Gelman, A.; Luokala, B. B.; Siclovan, T. M.; Kickelbick, G.; Vallant, T.; Hoffmann, H.; Pakula, T. Polymers at Interfaces: Using Atom Transfer Radical Polymerization in the Controlled Growth of Homopolymers and Block Copolymers from Silicon Surfaces in the Absence of Untethered Sacrificial Initiator. *Macromolecules* **1999**, *32*, 8716−8724.
(34) Dong, H.; Matyjaszewski, K. ARGET ATRP of 2-(Dimethylamino)ethyl Methacrylate as an Intrinsic Reducing Agent. *Macromolecules* **2008**, *41*, 6868−6870.
(35) Zhu, B.; Edmondson, S. Polydopamine-Melanin Initiators for Surface-Initiated ATRP. *Polymer* **2011**, *52*, 2141−2149.
(36) Kim, J.-B.; Huang, W.; Miller, M. D.; Baker, G. L.; Bruening, M. L. Kinetics of Surface-Initiated Atom Transfer Radical Polymerization. *J. Polym. Sci., Part A: Polym. Chem.* **2003**, *41*, 386−394.
(37) Bories-Azeau, X.; Armes, S. P.; van den Haak, H. J. W. Facile Synthesis of Zwitterionic Diblock Copolymers without Protecting Group Chemistry. *Macromolecules* **2004**, *37*, 2348−2352.